

Electronic structure of copper phthalocyanine from G_0W_0 calculationsNoa Marom,^{1,*} Xinguo Ren,² Jonathan E. Moussa,¹ James R. Chelikowsky,^{1,3} and Leeor Kronik⁴¹*Center for Computational Materials, Institute of Computational Engineering and Sciences, The University of Texas at Austin, Austin, Texas 78712, USA*²*Fritz-Haber-Institut der Max-Planck-Gesellschaft, Faradayweg 4-6, 14195, Berlin, Germany*³*Departments of Physics and Chemical Engineering, The University of Texas at Austin, Austin, Texas 78712, USA*⁴*Department of Materials and Interfaces, Weizmann Institute of Science, Rehovoth 76100, Israel*

(Received 11 August 2011; published 28 November 2011)

We present all-electron G_0W_0 calculations for the electronic structure of the organic semiconductor copper phthalocyanine, based on semilocal and hybrid density-functional theory (DFT) starting points. We show that G_0W_0 calculations improve the quantitative agreement with high resolution photoemission and inverse photoemission experiments. However, the extent of the improvement provided by G_0W_0 depends significantly on the choice of the underlying DFT functional, with the hybrid functional serving as a much better starting point than the semilocal one. In particular, strong starting-point dependence is observed in the energy positions of highly localized molecular orbitals. This is attributed to self-interaction errors (SIE), due to which the orbitals obtained from semilocal DFT do not approximate the quasi-particle (QP) orbitals as well as those obtained from hybrid DFT. Our findings establish the viability of the G_0W_0 approach for describing the electronic structure of metal-organic systems, given a judiciously chosen DFT-based starting point.

DOI: [10.1103/PhysRevB.84.195143](https://doi.org/10.1103/PhysRevB.84.195143)

PACS number(s): 73.22.-f

I. INTRODUCTION

In a molecular-solid form, copper phthalocyanine (CuPc), whose structure is schematically depicted in Fig. 1, is a highly stable organic semiconductor with a broad range of applications.¹ These include light-emitting diodes, solar cells, gas sensors, and thin-film transistors. It is even a candidate for single molecule devices. Owing to these applications, there is considerable interest in investigating its electronic structure, both experimentally^{2–19} and theoretically.^{2,3,10,16,20–31} Beyond its technological relevance, CuPc is a prototypical molecule representative of many metal-organic systems and therefore an excellent benchmark system for assessing computational methods.

To date, first principles studies of the electronic structure of CuPc have been dominated by density functional theory (DFT). In a previous study²⁶ some of us have shown that using DFT with semilocal or with hybrid functionals results in qualitatively different predictions regarding the nature and energy position of some of the frontier orbitals of CuPc, including the highest occupied molecular orbital (HOMO) and the lowest unoccupied molecular orbital (LUMO). We have further shown that hybrid functionals yield spectra that are in far better agreement with high resolution gas-phase ultraviolet photoemission spectroscopy (UPS) data.² The failure of semilocal functionals in this respect, which has subsequently been observed in other phthalocyanines and porphyrins,^{32–35} has been attributed to self-interaction errors (SIE).^{36–38} SIE arise from the spurious Coulomb interaction of an electron with itself in (semi-)local approximations to the exchange-correlation functional. Such errors do not occur in Hartree-Fock theory where they are explicitly canceled out by the exact (Fock) exchange term. It is thus possible to mitigate these errors by including a fraction of exact exchange, as done in hybrid functionals.^{38–41}

Still, even with modern hybrid functionals the agreement of calculated spectra with experiment is not perfect. Formally,

although the eigenvalues of a DFT calculation can serve as useful approximations for quasi-particle (QP) excitation energies,^{42–45} they are not rigorously equal to QP excitation energies. Even if semiquantitative agreement is achieved, the issue of the origin of finer differences between theory and experiment remains open. This is very much the case for CuPc. In particular one peak found in the high resolution UPS data (see the discussion of Fig. 4 below), which has been denoted as “peak F” in Ref. 2 and attributed experimentally to a Cu-derived state, did not find its match in the theoretical spectra. In the absence of further experimental or computational data, it was not possible to ascertain whether this reflects the remaining limitations of DFT in general or the employed functional in particular, or whether it stemmed from phenomena not considered in the calculation, such as final state or vibrational effects.²⁶

A logical step to take in order to answer this question is to turn to methods that compute QP excitation energies directly.⁴⁶ One of the most practical and widely employed methods is the many-body perturbation theory within the GW approximation,^{43,47–50} where G is the one-particle Green function and W is the dynamically screened Coulomb interaction. However, calculations based on GW can be prohibitively expensive, especially for larger molecules. Indeed, we are aware of only a limited number of previous GW calculations for organic molecules in the gas phase, e.g., Refs. 34, 40, and 51–67, most of which are quite recent. In particular only recently have GW-based calculations for the free-base phthalocyanine (H₂Pc) and related porphyrins begun to emerge.^{34,51,64} We are aware of only one GW study of a transition metal porphyrin derivative, but there the transition metal atom (Co) was replaced with a simpler metallic atom (Ca) for calculating the dynamically screened Coulomb interaction, W.⁶² None of these studies has employed a fully self-consistent GW.^{57,68–74} Often, a perturbative approach is used, where both the Green function and the screened Coulomb interaction are evaluated

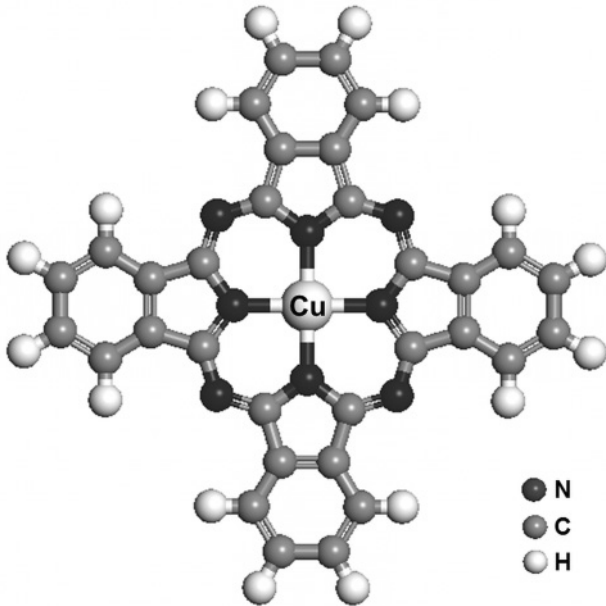


FIG. 1. Schematic illustration of a CuPc molecule.

using the underlying single-electron DFT orbitals. The final QP excitation energies are then obtained as a perturbative first-order correction to the DFT eigenvalues. This approach, which is used here, is known as G_0W_0 .

An additional simplification, employed in most G_0W_0 calculations, is to neglect off-diagonal terms in the self-energy operator. This amounts to assuming that the orbitals obtained from the DFT calculations mimic the QP wave function sufficiently well, in which case only the orbital energies need to be corrected.⁴³ Although this approximation is not universally valid (see, e.g., Ref. 52), it often yields excellent results. In particular GW studies of metal-free phthalocyanines and porphyrins,^{34,51,64} based on DFT with a semilocal functional as a starting point, have been found to yield satisfactory agreement with experiment.

Given the previously mentioned qualitative differences between semilocal and hybrid-functional DFT results for CuPc, it is not at all obvious that semilocal functionals would be a good starting point for GW in this case. Significant sensitivity of perturbative GW calculations to the choice of the DFT starting point has been noted before in solid-state systems. Examples include narrow-gap semiconductors, where semilocal functionals erroneously predict metallic behavior;^{75–78} large-gap semiconductors and insulators, where the QP gap underestimation in semilocal DFT calculations can be very large;^{76,79,80} and materials containing localized d -states, where semilocal DFT fails due to SIE.^{78,79,81,82}

Here, we explore whether G_0W_0 calculations for CuPc yield further quantitative agreement with experiment beyond that obtained from DFT calculations, and to what extent such further agreement depends on the DFT starting point. To this end, we perform perturbative G_0W_0 calculations based on both semilocal and hybrid-functional DFT calculations and compare our results to high-resolution gas-phase UPS data² and to thin film inverse photoemission spectroscopy (IPES) data.^{8,17} We find that the G_0W_0 calculations yield meaningful

improvements in the agreement with experimental results, as compared to those obtained from DFT. A detailed analysis reveals that these improvements are clearly discernible only upon comparison to high-resolution experimental data and are obtained only if a hybrid functional, rather than a semilocal one, is used as the starting point for the G_0W_0 calculation. We relate the observed starting point sensitivity to SIE effects, due to which the orbitals obtained from semilocal DFT do not approximate the QP orbitals as well as those obtained from hybrid DFT.

II. METHODS

A. Computational details

All calculations were performed using the all-electron numerical atom-centered orbital (NAO) code, FHI-aims.^{83,84} The NAO basis sets are grouped into a minimal basis, containing only basis functions for the core and valence electrons of the free atom, followed by four hierarchically constructed sets of additional basis functions, denoted by “*tier 1–4*.” A detailed description of these basis functions can be found in Ref. 83. The geometry of CuPc was relaxed using the generalized gradient approximation (GGA) of Perdew, Burke, and Ernzerhof (PBE)⁸⁵ with a *tier 2* basis set, which has been demonstrated to approach the basis set limit for ground-state GGA calculations and to be nearly free of basis set superposition errors.⁸³ The atomic zero-order regular approximation (ZORA)⁸³ was used to account for scalar relativistic effects during geometry relaxation.

G_0W_0 calculations were carried out using PBE as a semilocal functional starting point and the one-parameter PBE-based hybrid functional (PBEh, also known as PBE0), with 25% of Hartree-Fock exchange,⁸⁶ as a hybrid-functional starting point. The more accurate, but computationally more expensive, scaled ZORA⁸⁷ method was used to account for scalar relativistic effects in the single-point calculations that served as starting points for the G_0W_0 calculations. The spin state of CuPc was constrained to a doublet throughout using the formalism of Behler *et al.*^{88,89}

A detailed account of the all-electron implementation of GW in FHI aims has been given elsewhere.⁹⁰ Briefly, the implementation makes use of the resolution-of-identity (RI) technique, whereby a set of auxiliary basis functions is introduced to represent both the Coulomb potential and the noninteracting response function. This allows for efficient GW calculations with NAO basis functions. The RI accuracy and NAO basis set convergence have been benchmarked in Ref. 90. The self-energy is first calculated on the imaginary frequency axis and then analytically continued to the real frequency axis using a two-pole fitting procedure.⁹¹ As discussed in more detail below, GW calculations require a larger basis set than DFT calculations to achieve convergence with respect to the number of empty states. Here, GW calculations were performed using basis sets up to *tier 4*.

Performing GW calculations in an all-electron code has the advantage that possible pseudopotential errors are avoided. As discussed extensively in the literature, these errors, which do not affect ground-state DFT, may become significant in GW calculations if there is significant spatial overlap between core and valence wave-functions.^{74,92–99} In addition the compact

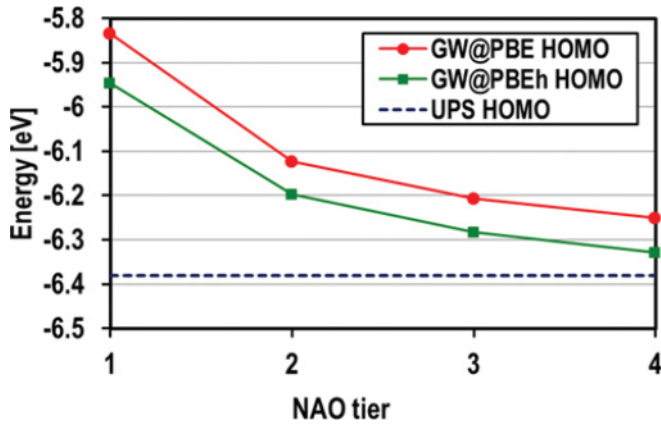


FIG. 2. (Color online) Quasi-particle HOMO energies obtained from G_0W_0 based on semilocal and hybrid starting points with increasingly large basis sets, compared to the experimental ionization potential.^{2,3,5}

and inherently local nature of the NAO basis functions leads to a more rapid convergence with the number of basis functions.¹⁰⁰ The fact that periodic boundary conditions need not be imposed in FHI-aims is another advantage for GW calculations of molecular systems, as there is no need for large regions of vacuum and there can be no artifacts due to spurious interactions between periodic replicas.

B. Basis set convergence

First, we examine the basis set convergence of our G_0W_0 calculations. The standard implementation of the GW self-energy contains an infinite sum over states,⁴³ which, in practice is carried out by a finite summation over a very large number of unoccupied states. This leads to notoriously slow convergence of GW calculations with respect to the number of unoccupied states.^{101,102} We conducted G_0W_0 calculations of CuPc, based on both PBE and PBEh (denoted throughout as GW@PBE and GW@PBEh, respectively), with increasingly large hierarchically constructed NAO basis sets¹⁰³ and compared the resulting QP HOMO energy to the experimental ionization potential (IP) value of 6.38 eV, obtained from gas phase UPS.^{2,3,5} The results are shown in Fig. 2. The largest change in the QP HOMO energy is from *tier 1* to *tier 2*. At the *tier 2* level, the QP HOMO energy is less than 0.3 eV away from experiment, whereas at the *tier 1* level the QP HOMO energy is ~ 0.5 eV higher than experiment. At the *tier 4* level, both the GW@PBE QP HOMO energy of 6.26 eV and the GW@PBEh QP HOMO of 6.31 eV are within ~ 0.1 eV from experiment. Our findings regarding basis set convergence are in agreement with those of Ren *et al.*⁹⁰ We also note that the spectra obtained at the *tier 2* level (not shown for brevity) were found to be qualitatively similar to those obtained at the *tier 4* level, with the difference being predominantly a rigid shift of the QP energies by ~ 0.2 eV. All results presented in the following were obtained

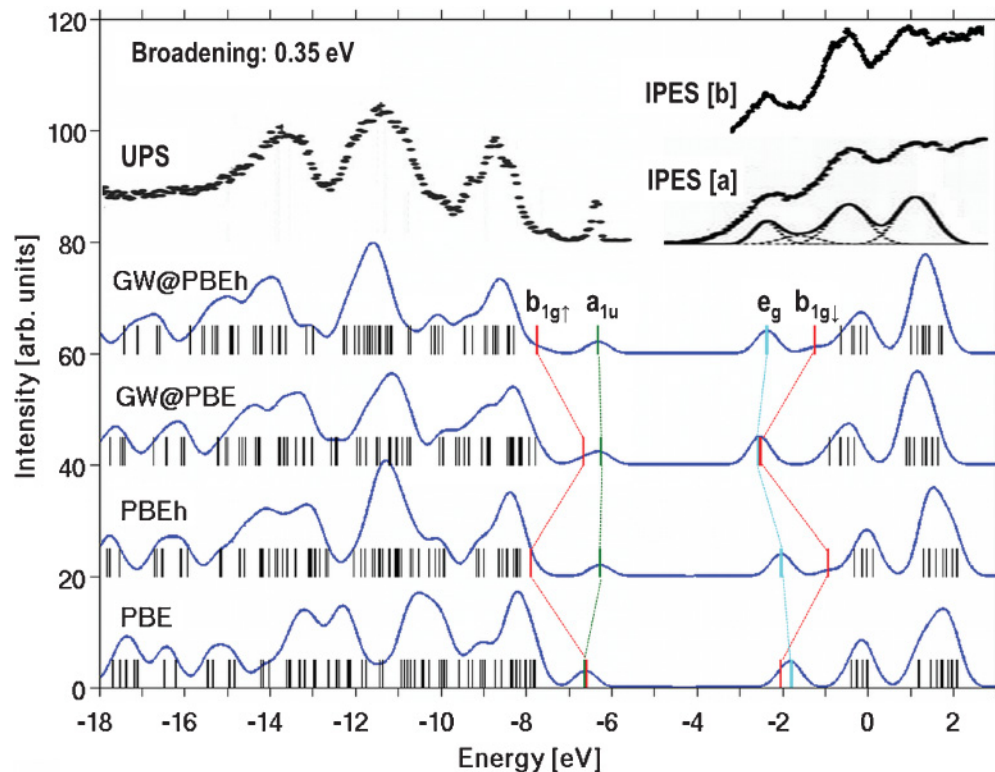


FIG. 3. (Color online) Calculated DFT and QP spectra, obtained from computed energy levels (shown as sticks) by broadening via convolution with a 0.35-eV-wide Gaussian, compared to gas phase UPS of Evangelista *et al.*² and to thin film IPES data of (a) Murdey *et al.*¹⁷ (shown with curve fitting results) and (b) Hill *et al.*⁸ DFT spectra were shifted so as to align the HOMO and LUMO levels with computed ionization potential and electron affinity values—see text for details. Experimental IPES spectra were shifted so as to align the LUMO peak with the computed GW@PBEh LUMO peak.

at the *tier 4* basis set level, which we consider to be adequately converged.

III. RESULTS AND DISCUSSION

The calculated spectra obtained with PBE, PBEh, GW@PBE, and GW@PBEh are shown in Fig. 3. They are compared to the gas phase UPS data of Evangelista *et al.*² and to two thin-film IPES experiments.^{8,17} We note that the comparison to additional gas phase UPS^{3,5} and IPES^{9,18} experiments is similar. The calculated spectra were obtained from computed single-particle energy levels, broadened by convolution with a 0.35-eV-wide Gaussian, in order to simulate the experimental resolution. It is important to understand how the energy levels in the different calculations were aligned. Because GW eigenvalues correspond directly to electron removal or addition energies, the GW energies were not modified. However, it is well known that for either PBE or PBEh the HOMO and LUMO do not correspond to the ionization potential or the electron affinity, respectively,⁴² causing an uncontrolled shift of the entire simulated photoemission curve. In theoretical simulations of photoemission from gas-phase clusters,^{104–106} this was remedied without fitting to experimental data by computing the ionization potential as the total energy difference between the neutral species and the cation¹⁰⁷ and rigidly shifting the filled-state eigenvalue spectrum such that the HOMO coincided with the computed ionization potential. Here, we employ the same procedure with the PBE and PBEh HOMO set at the total energy difference values of 6.57 and 6.27 eV, respectively. For the empty states a similar rigid shift was performed to align the LUMO with the computed electron affinity of 2.04 eV for both PBE and PBEh. The electron affinity was obtained by computing the total energy difference between the neutral species and the anion.¹⁰⁸ In addition, the experimental IPES data are for thin films where, due to polarization effects, the experimentally reported fundamental gap (i.e., the difference of the ionization potential and the electron affinity) of 3.1 eV is considerably smaller than the same gap in the isolated molecule. To preserve the computational gas-phase data, the *experimental* IPES spectra were shifted to align their leading peak with the leading peak of the GW@PBEh spectrum. We note that although cross-section effects can be taken into account to improve line-shape agreement between theory and experiment, as recently shown by Vogel *et al.* for CuPc,³ this was not included here because our focus is on peak positions.

As mentioned previously and discussed in Ref. 42, although QP energies are not given exactly by DFT eigenvalues, the latter are often a good approximation to QP energies. At the experimental resolution of the data in Fig. 3, this appears to be the case. All four calculated spectra exhibit the main features of the experimental spectra, namely, the HOMO peak followed by three broader peaks in the UPS data, and the three main peaks in the IPES data. The main difference between the DFT data and the GW data (or experiment) at this resolution is that the PBE spectrum is significantly compressed relative to experiment and the PBEh spectrum is still somewhat compressed. The two G_0W_0 spectra generally offer good quantitative agreement with experiment and with each other. For example, although the PBE and PBEh HOMO-LUMO

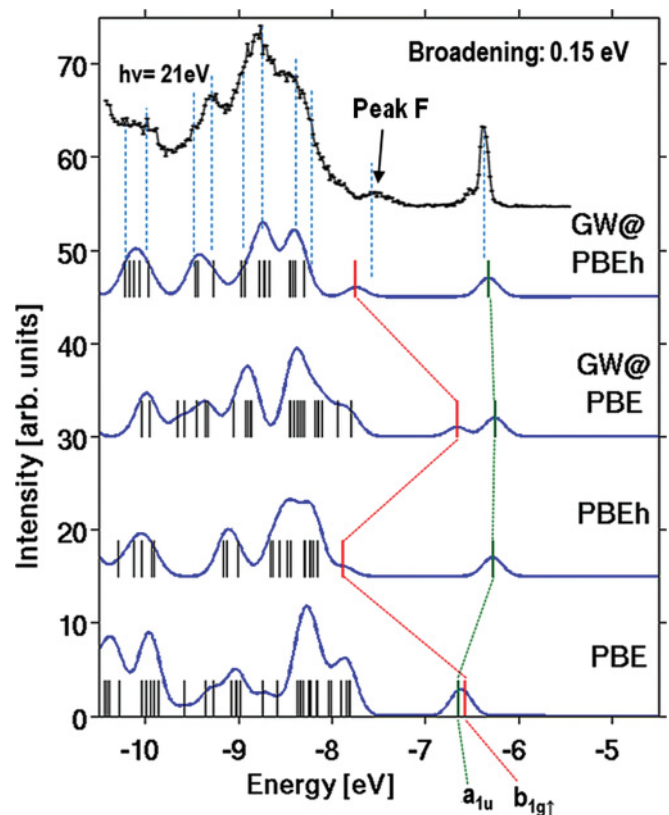


FIG. 4. (Color online) Calculated DFT and QP spectra, broadened by convolution with a 0.15-eV-wide Gaussian, compared to high-resolution gas phase UPS data.² The DFT spectra were shifted as in Fig. 3.

gaps are very different (1.12 eV and 2.33 eV, respectively), this leads to a difference of only 0.24 eV between the GW@PBE gap (3.70 eV) and the GW@PBEh gap (3.94 eV). Naively it would appear that (1) as known for inorganic semiconductors since the early days of G_0W_0 calculations,⁴³ the main effect of GW is to “shift and stretch” the DFT eigenvalues; (2) the DFT starting point is of little consequence for the final G_0W_0 result. We now demonstrate that neither conclusion holds up to scrutiny at a higher resolution.

The same theoretical spectra of Fig. 3, but broadened by convolution with a narrower, 0.15-eV-wide Gaussian, are compared in Fig. 4 to high-resolution gas phase UPS data² taken in the region of the HOMO peak and the first lower main peak. The recent gas phase UPS data of Ref. 3 exhibit the same peak positions and are not shown for brevity. Now that subfeatures of Fig. 3 can also be considered, the differences in accuracy of the theoretical spectra are revealed. We first focus on the position of the HOMO-1 peak. The positions of the a_{1u} and $b_{1g\uparrow}$ energy levels are illustrated in Figs. 3 and 4 (the corresponding orbitals are visualized in Fig. 5). As discussed previously,²⁶ owing to a large SIE in the PBE calculation, the $b_{1g\uparrow}$ orbital, which is highly localized around the Cu atom, is shifted to a higher energy. This shift causes PBE to predict an incorrect ordering of the frontier orbitals, where the $b_{1g\uparrow}$ orbital is the HOMO, located ~ 0.1 eV above the a_{1u} orbital.¹⁰⁹ This error is strongly reduced in the PBEh spectrum—the correct ordering is restored, and the overall agreement with

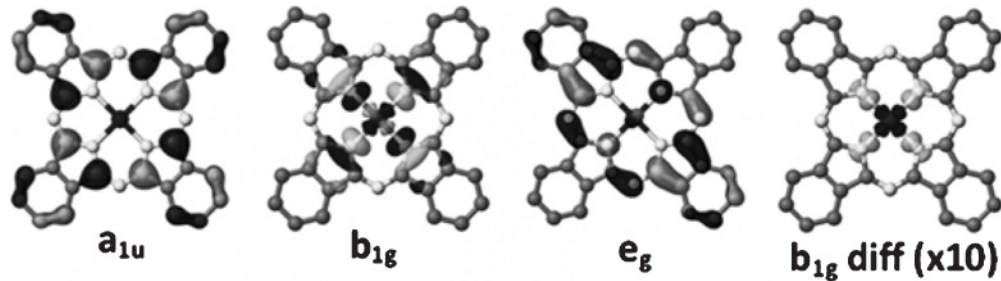


FIG. 5. Visualizations of selected leading molecular orbitals of CuPc. Also shown is the density difference between the $b_{1g\uparrow}$ orbitals obtained at the PBEh and PBE levels of theory, multiplied by a factor of ten for clarity of visualization. In the density difference plot, dark gray indicates a higher density in the PBE orbital and light gray indicates a higher density in the PBEh orbital.

experiment is much improved. This is consistent with the higher SIE attributed to the localized $b_{1g\uparrow}$ orbital, as compared to the a_{1u} orbital, which is delocalized over the organic macrocycle.

Similarly to PBEh, GW@PBE reorders the $b_{1g\uparrow}$ and a_{1u} orbitals, correctly making the a_{1u} orbital the HOMO. However, the $b_{1g\uparrow}$ orbital is placed only ~ 0.4 eV below the a_{1u} orbital, leading to a doubling of the first peak of the simulated spectrum, which is in disagreement with experiment. The GW@PBEh spectrum is significantly better—not only is the correct orbital-ordering obtained, but the $b_{1g\uparrow}$ orbital is found ~ 1.4 eV below the a_{1u} orbital. At this position, the $b_{1g\uparrow}$ related feature is in very close agreement with the position of “peak F” in the UPS data. Furthermore, this is consistent with the attribution of “peak F” to a Cu-derived orbital in the experimental work of Evangelista *et al.*² Importantly, in the PBEh spectrum, the $b_{1g\uparrow}$ orbital is somewhat lower, lying ~ 1.6 eV below the a_{1u} HOMO. At this position, and with the theoretical broadening used to simulate experiment, the $b_{1g\uparrow}$ orbital forms a shoulder on the second peak of the simulated spectrum, rather than a separate peak, so that “peak F” could not be unequivocally identified from the PBEh data.

Our calculations also yield significant differences between GW@PBE and GW@PBEh in the position of the LUMO and LUMO + 1 orbitals, as shown in Fig. 3. Visualization of the LUMO and LUMO + 1 orbitals, given in Fig. 5, reveals that these differences are related to the energy position of the empty counterpart of the spin-split b_{1g} orbital, $b_{1g\downarrow}$. The PBE calculation erroneously predicts this orbital to be the LUMO, lying ~ 0.25 eV below the non-spin-split e_g orbital. We have previously postulated that because the SIE shifts the occupied $b_{1g\uparrow}$ orbital to a higher energy, it also shifts its empty counterpart, $b_{1g\downarrow}$, to a lower energy, with the overall spin-split energy severely underestimated.²⁶ Just as

for the filled states, the correct ordering is restored by PBEh, which places the $b_{1g\downarrow}$ orbital ~ 1.1 eV above the e_g LUMO. Similarly to the valence spectrum, the empty-state spectrum is not satisfactorily corrected by GW@PBE. In the GW@PBE spectrum the $b_{1g\downarrow}$ orbital is essentially degenerate with the e_g LUMO, lying only ~ 0.03 eV above it. In contrast the GW@PBEh calculation maintains the PBEh orbital ordering, with a similar energy difference between the $b_{1g\downarrow}$ orbital and the e_g LUMO. At this position, the $b_{1g\downarrow}$ orbital is in close agreement with the position of a low intensity peak in the experimental spectrum, identified by Murdey *et al.*¹⁷ via curve fitting (shown in Fig. 3) and assigned by them to a Cu-derived b_{1g} state. This indicates yet again that PBEh is superior to PBE as a starting point for G_0W_0 , not only with respect to the occupied states, but also with respect to the empty ones.

The deficiency of GW@PBE, as compared to either GW@PBEh or experiment, indicates that the spurious upward shift of the $b_{1g\uparrow}$ orbital and the corresponding downward shift of the $b_{1g\downarrow}$ orbital in the PBE calculation are only partially corrected. This suggests that in this case the PBE starting point is too far from the correct solution to result in an accurate perturbative G_0W_0 calculation. In contrast the GW@PBEh correction to the energy of the $b_{1g\uparrow}$ orbital is only slightly less negative than that for the a_{1u} orbital, indicating that PBEh is a much better starting point with respect to the position of the $b_{1g\uparrow}$ orbital. To identify the origin of this starting point sensitivity, additional G_0W_0 calculations were performed, where PBEh was used to calculate the dynamic dielectric function ϵ in an otherwise PBE-based GW calculation, and vice versa. A *tier 2* basis set was employed for these calculations. The resulting QP energies of the frontier orbitals of CuPc are shown in Table I.

Evidently, the QP energies of the localized $b_{1g\uparrow,\downarrow}$ orbitals depend more strongly on G and W than on ϵ . Therefore, one

TABLE I. QP energies (in eV) of the frontier orbitals of CuPc, obtained using different combinations of DFT functionals for the GW QP orbitals and calculation of the dielectric matrix ϵ . These calculations were performed with a *tier 2* basis set.

GW	ϵ	$b_{1g\uparrow}$	$a_{1u\uparrow}$	$a_{1u\downarrow}$	$e_{g\uparrow}$	$e_{g\downarrow}$	$b_{1g\downarrow}$
PBE	PBE	-6.35	-6.12	-6.13	-2.37	-2.35	-2.19
PBEh	PBEh	-7.49	-6.20	-6.21	-2.22	-2.19	-0.92
PBE	PBEh	-6.66	-6.16	-6.17	-2.278	-2.25	-1.94
PBEh	PBE	-7.27	-6.16	-6.17	-2.29	-2.27	-1.23

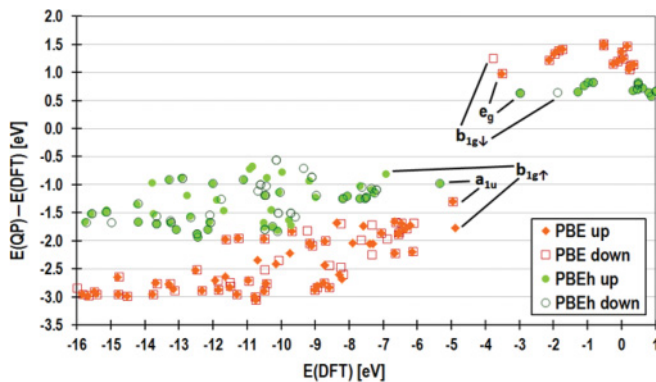


FIG. 6. (Color online) QP corrections as a function of DFT energies for both the PBE the PBEh starting points.

cannot ascribe the unsatisfactory results of the GW@PBE calculations merely to overscreening, resulting from an overestimated polarization due to the small HOMO-LUMO gap of PBE. This means that for highly localized orbitals that carry a large SIE, the orbitals obtained from semilocal DFT are not a satisfactory approximation to the QP orbitals. This conclusion is further supported by calculating the electron-density difference between the $b_{1g\uparrow}$ orbital obtained from PBEh and from PBE, visualized in Fig. 5. The difference in the density is small compared to the densities themselves and has to be magnified by a factor of 10 with respect to the other orbital densities visualized in Fig. 5. Still, such small differences are known to be significant for GW calculations.⁸¹ For the $b_{1g\uparrow}$ orbital, the difference between PBEh and PBE amounts to a lower density around the Cu atom and a higher density around the neighboring N atoms for PBEh. In comparison the differences between the PBEh and PBE densities of the $a_{1u\uparrow}$ and $e_{g\uparrow}$ orbitals are invisible even at this magnification. This is consistent with the weaker starting point dependence of the QP energies of these orbitals. The strong dependence of the QP-correction of the DFT energies on the spatial distribution of the KS orbitals, rather than just on the KS eigenvalues, may indicate that partial self-consistency only in the eigenvalues would not be sufficient to remedy severe SIE issues.

Our findings are reminiscent of those reported in Refs. 78, 79, 81, and 82 for several semiconductors. There, it was shown that the underbinding of the d -band by semilocal functionals owing to SIE leads to changes in hybridization. Similarly to the case of CuPc, the inadequacy of the semilocal starting point for these semiconductors carries over to G_0W_0 calculations and a hybrid starting point proves to be superior. Interestingly, although both the b_{1g} and the e_g orbitals have Cu- d contributions, this leads to a change in hybridization and starting point sensitivity only for the b_{1g} orbital. We also note that this issue is not restricted to systems with d -orbitals and may arise in any system afflicted with SIE. For example, the starting point sensitivity observed for, cytosine, uracil, and isonicotinic acid is caused by SIE in orbitals associated with the localized nitrogen lone pair.^{60,66}

So far we have focused mostly on the spin-split b_{1g} orbital as an important special case. Figure 6 exhibits the QP corrections to the PBE and PBEh for a wider range of energies. Generally,

the QP corrections over the PBEh starting point are smaller than the QP energy corrections over the PBE starting point, making PBEh a better starting point. Contrary to the “shift and stretch” G_0W_0 corrections often observed in typical inorganic semiconductors,⁴³ the QP corrections to the different orbitals found here are quite scattered and do not form an obvious straight line. We attribute this to the different degree of localization and resulting SIE for each orbital.^{37,38} In such cases a simple stretch of the DFT spectrum is not sufficient to compensate for SIE. This demonstrates clearly that SIE-related differences in the DFT starting point are generally carried over to the G_0W_0 calculations.

IV. CONCLUSIONS

We conducted G_0W_0 calculations for the electronic structure of CuPc, based on semi-local (PBE) and hybrid (PBEh) DFT starting points and compared the results to available gas phase UPS and thin film IPES data. We found that GW@PBEh yields excellent agreement with experimental results, especially with respect to the positions of the peaks associated with the Cu-derived b_{1g} orbital, but that GW@PBE does not. We attribute the observed starting point sensitivity of G_0W_0 calculations to SIE in the semilocal DFT calculations, which partly carry over to the perturbative G_0W_0 results. The localization and hybridization of orbitals exhibiting significant SIE are affected, making them unsatisfactory approximations to the QP orbitals. This problem cannot be remedied by correction schemes that only shift the DFT eigenvalues without changing the spatial distribution of the orbitals and would require off-diagonal correction terms that could be prohibitively expensive computationally. In such cases the orbitals obtained from hybrid DFT provide a better approximation to the QP orbitals and thus a more reliable starting point for G_0W_0 calculations. Our findings establish the viability of the G_0W_0 approach for describing the electronic structure of metal-organic systems, given a judiciously chosen DFT-based starting point.

ACKNOWLEDGMENTS

We thank Steven G. Louie (UC Berkeley) for illuminating discussions. We acknowledge support from the National Science Foundation under Grant Nos. DMR-0941645 and OCI-1047997 and from the US Department of Energy under Grant No. DE-SC0001878. Computational resources were provided by the National Energy Research Scientific Computing Center (NERSC) and the Oak Ridge Leadership Computing Facility (OLCF), located in the National Center for Computational Sciences at Oak Ridge National Laboratory. The National Science Foundation provided computational resources through TeraGrid at the Texas Advanced Computing Center (TACC) under Grant No. TG-DMR090026. Work at the Weizmann Institute was supported by the Israel Science Foundation, by the Lise Meitner Center for Computational Chemistry, and by the historical generosity of the Perlman Family. One of us (JRC) would like to thank support from the Welch Foundation under Grant No. F-1708.

*Corresponding author: noa@ices.utexas.edu

- ¹K. M. Kadish, K. M. Smith, and R. Guilard, *The Porphyrin Handbook, Vol 19: Applications of Phthalocyanines* (Academic Press San Diego, California, 2003).
- ²F. Evangelista, V. Carravetta, G. Stefani, B. Jansik, M. Alagia, S. Stranges, and A. Ruocco, *J. Chem. Phys.* **126**, 124709 (2007).
- ³M. Vogel, F. Schmitt, J. Sauther, B. Baumann, A. Altenhof, S. Lach, and C. Ziegler, *Analytical and Bioanalytical Chemistry* **400**, 673 (2011).
- ⁴T. Schwieger, H. Peisert, M. S. Golden, M. Knupfer, and J. Fink, *Phys. Rev. B* **66**, 155207 (2002).
- ⁵J. Berkowitz, *J. Chem. Phys.* **70**, 2819 (1979).
- ⁶S. Kera, H. Yamane, I. Sakuragi, K. K. Okudaira, and N. Ueno, *Chem. Phys. Lett.* **364**, 93 (2002).
- ⁷P. I. Djurovich, E. I. Mayo, S. R. Forrest, and M. E. Thompson, *Org. Electron.* **10**, 515 (2009).
- ⁸I. G. Hill, A. Kahn, Z. G. Soos, and J. R. A. Pascal, *Chem. Phys. Lett.* **327**, 181 (2000).
- ⁹H. Ding and Y. Gao, *Appl. Phys. Lett.* **92**, 053309 (2008).
- ¹⁰M. Grobosch, B. Mahns, C. Loose, R. Friedrich, C. Schmidt, J. Kortus, and M. Knupfer, *Chem. Phys. Lett.* **505**, 122 (2011).
- ¹¹F. Schmitt, J. Sauther, S. Lach, and C. Ziegler, *Analytical and Bioanalytical Chemistry* **400**, 665 (2011).
- ¹²L. Lozzi and S. Santucci, *J. Chem. Phys.* **134**, 114709 (2011).
- ¹³W. D. Dou, S. P. Huang, R. Q. Zhang, and C. S. Lee, *J. Chem. Phys.* **134**, 094705 (2011).
- ¹⁴K. Akaïke, A. Opitz, J. Wagner, W. Brutting, K. Kanai, Y. Ouchi, and K. Seki, *Org. Electron.* **11**, 1853 (2010).
- ¹⁵J. Xiao and P. A. Dowben, *J. Mater. Chem.* **19**, 2172 (2009).
- ¹⁶V. Y. Aristov, O. V. Molodtsova, V. V. Maslyuk, D. V. Vylikh, V. M. Zhilin, Y. A. Ossipyan, T. Bredow, I. Mertig, and M. Knupfer, *J. Chem. Phys.* **128**, 034703 (2008).
- ¹⁷R. Murdey, N. Sato, and M. Bouvet, *Mol. Cryst. Liquid Cryst.* **455**, 211 (2006).
- ¹⁸M. L. M. Rocco, K. H. Frank, P. Yannoulis, and E. E. Koch, *J. Chem. Phys.* **93**, 6859 (1990).
- ¹⁹M. Grobosch, C. Schmidt, R. Kraus, and M. Knupfer, *Org. Electron.* **11**, 1483 (2010).
- ²⁰B. Bialek, I. G. Kim, and J. I. Lee, *Thin Solid Films* **436**, 107 (2003).
- ²¹D. C. Li, Z. H. Peng, L. Z. Deng, W. F. Shen, and Y. H. Zhou, *Vib. Spectrosc.* **39**, 191 (2005).
- ²²A. Rosa and E. J. Baerends, *Inorg. Chem.* **33**, 584 (1994).
- ²³N. Shi and R. Ramprasad, *Phys. Rev. B* **75**, 155429 (2007).
- ²⁴A. Calzolari, A. Ferretti, and M. B. Nardelli, *Nanotechnology* **18**, 424013 (2007).
- ²⁵M. S. Liao and S. Scheiner, *J. Chem. Phys.* **114**, 9780 (2001).
- ²⁶N. Marom, O. Hod, G. E. Scuseria, and L. Kronik, *J. Chem. Phys.* **128**, 164107 (2008).
- ²⁷Y. T. Yang, Y. M. Yang, F. G. Wu, and Z. G. Wei, *Solid State Commun.* **148**, 559 (2008).
- ²⁸F. Flores, J. Ortega, and H. Vazquez, *Phys. Chem. Chem. Phys.* **11**, 8658 (2009).
- ²⁹X. Shen, L. L. Sun, Z. L. Yi, E. Benassi, R. X. Zhang, Z. Y. Shen, S. Sanvito, and S. M. Hou, *Phys. Chem. Chem. Phys.* **12**, 10805 (2010).
- ³⁰D. D. O'Regan, M. C. Payne, and A. A. Mostofi, *Phys. Rev. B* **83**, 245124 (2011).
- ³¹W. Wu, A. Kerridge, A. H. Harker, and A. J. Fisher, *Phys. Rev. B* **77**, 184403 (2008).
- ³²N. Marom and L. Kronik, *Appl. Phys. a-Mater.* **95**, 159 (2009).
- ³³D. Stradi, C. Diaz, F. Martin, and M. Alcami, *Theor. Chem. Acc.* **128**, 497 (2011).
- ³⁴M. Palummo, C. Hogan, F. Sottile, P. Bagala, and A. Rubio, *J. Chem. Phys.* **131**, 084102 (2009).
- ³⁵B. Brena, C. Puglia, M. de Simone, M. Coreno, K. Tarafder, V. Feyer, R. Banerjee, E. Gothelid, B. Sanyal, P. M. Oppeneer, and O. Eriksson, *J. Chem. Phys.* **134**, 074312 (2011).
- ³⁶J. P. Perdew and A. Zunger, *Phys. Rev. B* **23**, 5048 (1981).
- ³⁷T. Körzdörfer, S. Kümmel, N. Marom, and L. Kronik, *Phys. Rev. B* **79**, 201205 (2009); **82**, 129903 (2010).
- ³⁸T. Körzdörfer, *J. Chem. Phys.* **134**, 094111 (2011).
- ³⁹T. Körzdörfer and S. Kümmel, *Phys. Rev. B* **82**, 155206 (2010).
- ⁴⁰N. Dori, M. Menon, L. Kilian, M. Sokolowski, L. Kronik, and E. Umbach, *Phys. Rev. B* **73**, 195208 (2006).
- ⁴¹F. Rissner, D. A. Egger, A. Natan, T. Körzdörfer, S. Kümmel, L. Kronik, and E. Zojer, *J. Am. Chem. Soc.* **133**, 18634 (2011).
- ⁴²S. Kümmel and L. Kronik, *Rev. Mod. Phys.* **80**, 3 (2008).
- ⁴³M. S. Hybertsen and S. G. Louie, *Phys. Rev. B* **34**, 5390 (1986).
- ⁴⁴D. P. Chong, O. V. Gritsenko, and E. J. Baerends, *J. Chem. Phys.* **116**, 1760 (2002).
- ⁴⁵O. V. Gritsenko and E. J. Baerends, *J. Chem. Phys.* **117**, 9154 (2002).
- ⁴⁶It is also possible to extract a photoemission spectrum from time-dependent DFT (TDDFT). However, unlike the QP energies of GW, which correspond to charged excitations of the neutral species and are thus directly comparable to PES, the corresponding TDDFT excitations are neutral excitations of the cation that need to be added to the ionization potential. See, e.g., O. T. Ehrler, J. M. Weber, F. Furche, M. M. Kappes, *Phys. Rev. Lett.* **91**, 113006 (2007); M. Mundt and S. Kümmel, *Phys. Rev. B* **76**, 035413 (2007).
- ⁴⁷L. Hedin, *Phys. Rev.* **139**, A796 (1965).
- ⁴⁸G. Onida, L. Reining, and A. Rubio, *Rev. Mod. Phys.* **74**, 601 (2002).
- ⁴⁹F. Aryasetiawan and O. Gunnarsson, *Rep. Prog. Phys.* **61**, 237 (1998).
- ⁵⁰W. G. Aulbur, L. Jonsson, and J. W. Wilkins, in *Solid State Physics: Advances in Research and Applications, Vol. 54*, edited by, M. Ehrenreich and F. Spaepen (Academic Press Inc., San Diego, California, 2000), p. 1.
- ⁵¹X. Blase, C. Attaccalite, and V. Olevano, *Phys. Rev. B* **83**, 115103 (2011).
- ⁵²J. C. Grossman, M. Rohlfing, L. Mitas, S. G. Louie, and M. L. Cohen, *Phys. Rev. Lett.* **86**, 472 (2001).
- ⁵³M. L. Tiago and J. R. Chelikowsky, *Solid State Commun.* **136**, 333 (2005).
- ⁵⁴J. B. Neaton, M. S. Hybertsen, and S. G. Louie, *Phys. Rev. Lett.* **97**, 216405 (2006).
- ⁵⁵P. Umari, G. Stenuit, and S. Baroni, *Phys. Rev. B* **81**, 115104 (2010).
- ⁵⁶Y. C. Ma, M. Rohlfing, and C. Molteni, *Phys. Rev. B* **80**, 241405 (2009).
- ⁵⁷C. Rostgaard, K. W. Jacobsen, and K. S. Thygesen, *Phys. Rev. B* **81**, 085103 (2010).

- ⁵⁸P. Umari, C. Castellarin-Cudia, V. Feyer, G. Di Santo, P. Borghetti, L. Sangaletti, G. Stenuit, and A. Goldoni, *Phys. Status Solidi B* **248**, 960 (2011).
- ⁵⁹X. F. Qian, P. Umari, and N. Marzari, *Phys. Rev. B* **84**, 075103 (2011).
- ⁶⁰C. Faber, C. Attaccalite, V. Olevano, E. Runge, and X. Blase, *Phys. Rev. B* **83**, 115123 (2011).
- ⁶¹J. M. Garcia-Lastra and K. S. Thygesen, *Phys. Rev. Lett.* **106**, 187402 (2011).
- ⁶²L. da Silva, M. L. Tiago, S. E. Ulloa, F. A. Reboredo, and E. Dagotto, *Phys. Rev. B* **80**, 155443 (2009).
- ⁶³M. L. Tiago, P. R. C. Kent, R. Q. Hood, and F. A. Reboredo, *J. Chem. Phys.* **129**, 084311 (2008).
- ⁶⁴G. Stenuit, C. Castellarin-Cudia, O. Plekan, V. Feyer, K. C. Prince, A. Goldoni, and P. Umari, *Phys. Chem. Chem. Phys.* **12**, 10812 (2010).
- ⁶⁵X. Blase and C. Attaccalite, *Appl. Phys. Lett.* **99**, 171909 (2011).
- ⁶⁶N. Marom, J. E. Moussa, X. Ren, A. Tkatchenko, and J. R. Chelikowsky, *Phys. Rev. B* (in press).
- ⁶⁷N. Sai, M. L. Tiago, J. R. Chelikowsky, and F. A. Reboredo, *Phys. Rev. B* **77**, 161306 (2008).
- ⁶⁸T. Kotani and M. van Schilfgaarde, *Phys. Rev. B* **81**, 125201 (2010).
- ⁶⁹A. Svane, N. E. Christensen, M. Cardona, A. N. Chantis, M. van Schilfgaarde, and T. Kotani, *Phys. Rev. B* **81**, 245120 (2010).
- ⁷⁰A. Svane, N. E. Christensen, I. Gorczyca, M. van Schilfgaarde, A. N. Chantis, and T. Kotani, *Phys. Rev. B* **82**, 115102 (2010).
- ⁷¹F. Bruneval, *Phys. Rev. Lett.* **103**, 176403 (2009).
- ⁷²F. Bruneval, N. Vast, and L. Reining, *Phys. Rev. B* **74**, 045102 (2006).
- ⁷³M. Strange, C. Rostgaard, H. Hakkinen, and K. S. Thygesen, *Phys. Rev. B* **83**, 115108 (2011).
- ⁷⁴W. Ku and A. G. Eguiluz, *Phys. Rev. Lett.* **89**, 126401 (2002).
- ⁷⁵A. Qteish, P. Rinke, M. Scheffler, and J. Neugebauer, *Phys. Rev. B* **74**, 245208 (2006).
- ⁷⁶P. Rinke, A. Qteish, J. Neugebauer, and M. Scheffler, *Phys. Status Solidi B* **245**, 929 (2008).
- ⁷⁷P. Rinke, M. Scheffler, A. Qteish, M. Winkelkemper, D. Bimberg, and J. Neugebauer, *Appl. Phys. Lett.* **89**, 161919 (2006).
- ⁷⁸C. Rodl, F. Fuchs, J. Furthmuller, and F. Bechstedt, *Phys. Rev. B* **79**, 235114 (2009).
- ⁷⁹F. Fuchs and F. Bechstedt, *Phys. Rev. B* **77**, 155107 (2008).
- ⁸⁰W. G. Aulbur, M. Städele, and A. Görling, *Phys. Rev. B* **62**, 7121 (2000).
- ⁸¹P. Rinke, A. Qteish, J. Neugebauer, C. Freysoldt, and M. Scheffler, *New J. Phys.* **7**, 126 (2005).
- ⁸²F. Fuchs, J. Furthmuller, F. Bechstedt, M. Shishkin, and G. Kresse, *Phys. Rev. B* **76**, 115109 (2007).
- ⁸³V. Blum, R. Gehrke, F. Hanke, P. Havu, V. Havu, X. Ren, K. Reuter, and M. Scheffler, *Comput. Phys. Commun.* **180**, 2175 (2009).
- ⁸⁴V. Havu, V. Blum, P. Havu, and M. Scheffler, *J. Comput. Phys.* **228**, 8367 (2009).
- ⁸⁵J. P. Perdew, K. Burke, and M. Ernzerhof, *Phys. Rev. Lett.* **77**, 3865 (1996); **78**, 1396 (1997).
- ⁸⁶C. Adamo and V. Barone, *J. Chem. Phys.* **110**, 6158 (1999).
- ⁸⁷E. v. Lenthe, E. J. Baerends, and J. G. Snijders, *J. Chem. Phys.* **101**, 9783 (1994).
- ⁸⁸J. Behler, B. Delley, S. Lorenz, K. Reuter, and M. Scheffler, *Phys. Rev. Lett.* **94**, 036104 (2005).
- ⁸⁹J. Behler, B. Delley, K. Reuter, and M. Scheffler, *Phys. Rev. B* **75**, 115409 (2007).
- ⁹⁰X. Ren, P. Rinke, V. Blum, J. Wieferink, A. Tkatchenko, A. Sanfilippo, K. Reuter, and M. Scheffler, to be published.
- ⁹¹H. N. Rojas, R. W. Godby, and R. J. Needs, *Phys. Rev. Lett.* **74**, 1827 (1995).
- ⁹²R. Gomez-Abal, X. Z. Li, M. Scheffler, and C. Ambrosch-Draxl, *Phys. Rev. Lett.* **101**, 106404 (2008).
- ⁹³C. Friedrich, A. Schindlmayr, S. Blügel, and T. Kotani, *Phys. Rev. B* **74**, 045104 (2006).
- ⁹⁴M. Shishkin and G. Kresse, *Phys. Rev. B* **74**, 035101 (2006).
- ⁹⁵M. L. Tiago, S. Ismail-Beigi, and S. G. Louie, *Phys. Rev. B* **69**, 125212 (2004).
- ⁹⁶M. van Schilfgaarde, T. Kotani, and S. V. Faleev, *Phys. Rev. B* **74**, 245125 (2006).
- ⁹⁷K. Delaney, P. Garcia-Gonzalez, A. Rubio, P. Rinke, and R. W. Godby, *Phys. Rev. Lett.* **93**, 249701 (2004).
- ⁹⁸W. Ku and A. G. Eguiluz, *Phys. Rev. Lett.* **93**, 249702 (2004).
- ⁹⁹E. Luppi, H. C. Weissker, S. Bottaro, F. Sottile, V. Veniard, L. Reining, and G. Onida, *Phys. Rev. B* **78**, 245124 (2008).
- ¹⁰⁰For an additional perspective on the convergence of G_0W_0 calculations using local basis sets and plane waves, see G. Samsonidze, M. Jain, J. Deslippe, M. L. Cohen, and S. G. Louie, *Phys. Rev. Lett.* **107**, 186404 (2011).
- ¹⁰¹B. C. Shih, Y. Xue, P. H. Zhang, M. L. Cohen, and S. G. Louie, *Phys. Rev. Lett.* **105**, 146401 (2010).
- ¹⁰²C. Friedrich, M. C. Muller, and S. Blügel, *Phys. Rev. B* **83**, 081101 (2011).
- ¹⁰³For CuPc, the *tier 1* NAO basis set contains 680 basis functions, the *tier 2* basis set contains 1867 basis functions, the *tier 3* basis set contains 2772 basis functions, and the *tier 4* basis set contains 3752 basis functions.
- ¹⁰⁴L. Kronik, R. Fromherz, E. Ko, G. Ganteför, and J. R. Chelikowsky, *Nat. Mater.* **1**, 49 (2002).
- ¹⁰⁵M. Moseler, B. Huber, H. Häkkinen, U. Landman, G. Wrigge, M. A. Hoffmann, and B. von Issendorff, *Phys. Rev. B* **68**, 165413 (2003).
- ¹⁰⁶O. Guliamov, L. Kronik, and K. A. Jackson, *J. Chem. Phys.* **123**, 204312 (2005).
- ¹⁰⁷We note that the PBE cation is a closed-shell singlet, while the PBEh cation is an open-shell singlet because the orbital ordering predicted by these functionals is such that for PBE the electron is removed from the singly occupied $b_{1g\uparrow}$ orbital, whereas for PBEh the electron is removed from the doubly occupied a_{1u} orbital.
- ¹⁰⁸The anion is a triplet with both PBE and PBEh.
- ¹⁰⁹In Ref. 26, a different orbital ordering has been reported for a PBE calculation of CuPc, with the a_{1u} orbital as the HOMO and the $b_{1g\uparrow}$ orbital as the HOMO-1. This difference is a result of the more converged basis set used here.